Theoretical Study of the Reaction Mechanism of Fe Atoms with H_2O, H_2S, O_2 and H^+

Alexander M. Mebel*,† and Der-Yan Hwang*,‡

Institute of Atomic and Molecular Sciences, Academia Sinica, P.O. Box 23-166, Taipei 10764, Taiwan, and Department of Chemistry, Tamkang University, Tamsui 25137, Taiwan

Density functional B3LYP/6-31G**, B3LYP/6-311G**, B3LYP/6-311+G(3df,2p), and ab initio CCSD(T)/6-311G** calculations showed the reaction of free iron atoms with water in the ground quintet electronic state to proceed by the formation of a weakly bound $Fe-OH_2$ molecular complex. The complex is slightly unbound at the CCSD(T)/6-311G** level but stable according to density functional calculations and can isomerize to the HFeOH molecule, overcoming a barrier of 15−33 kcal/mol (with respect to the reactants), but further decomposition of HFeOH to FeO and H_2 is hindered by a high barrier. In the presence of protons (in acidic environment), iron atoms can easily attach H^+ with formation of the quintet FeH^+ molecules. The reaction of these molecules with water, $q\text{-}FeH^+ + H_2O \rightarrow q\text{-}HFeOH_2+ \rightarrow q\text{-}FeOH^+ + H_2$, is exothermic and occurs without activation barrier. In solution, $q\text{-}FeOH^+$ may attach another proton (if the Coulomb repulsion barrier between the two ions can be overcome) and dissociate to $q\text{-}Fe^{2+}$ and H_2O, so the water molecule assists oxidation of a neutral iron atom to Fe^{2+}, and two protons can be converted into molecular hydrogen transferring their charge to Fe. The FeH^+ molecules are also shown to readily react with molecular oxygen, producing $FeOOH^+$ without energy barrier. The $FeH^+ + O_2$ reaction is more facile than the reaction of FeH^+ with water due to higher overall exothermicity (68−88 kcal/mol vs 20−34 kcal/mol for $FeH^+ + H_2O \rightarrow FeOH^+ + H_2$) and a lower barrier for the intermediate reaction step (14−17 vs 35−46 kcal/mol), which can be rate-determining if the reaction occurs in solution. The reaction mechanism involving sequential $Fe(^5D) + H^+ \rightarrow q\text{-}FeH^+$, $q\text{-}FeH^+ + O_2 \rightarrow q\text{-}HFeO_2+ \rightarrow q\text{-}FeOOH^+$ reactions, followed by dissociation of $q\text{-}FeOOH^+$ in solution yielding Fe^{2+}, may be relevant to the first step of rusting. The calculations showed that electronically excited triplet iron atoms are more reactive with H_2O. The triplet $Fe + H_2O \rightarrow Fe-OH_2 \rightarrow HFeOH$ reaction is exothermic and has its transition state lying lower in energy than the reactants. No triplet-quintet intersystem crossing was found along the reaction pathway. The mechanism for the $Fe + H_2S$ reaction in the ground quintet electronic state is found to be similar to that for the reaction with water, but the critical barrier for the formation of the HFeSH intermediate is lower. Because of the reduced endothermicity of the $Fe + H_2S \rightarrow FeS + H_2$ reaction and lower reaction barriers, the reaction of iron atoms with H_2S is more likely to yield iron sulfide and molecular hydrogen than the reaction with water to produce $FeO + H_2$.
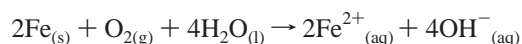
1. Introduction

Corrosion causes enormous damage to buildings, bridges, ships, and cars. Although the reactions involved are quite complex and not completely understood, the main steps are believed to be as follows.[1] A region of the metals' surface serves as the anode, where the following oxidation occurs:

$$Fe_{(s)} \rightarrow Fe^{2+}_{(aq)} + 2e^-$$
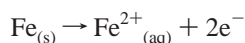
The electrons given up by iron reduce atmospheric oxygen to water at the cathode, which is another region of the same metal surface

$$O_{2(g)} + 4H_2O_{(l)} + 4e^- \rightarrow 4OH^-_{(aq)}$$
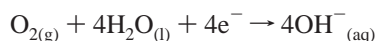
The overall redox reaction is

$$2Fe_{(s)} + O_{2(g)} + 4H_2O_{(l)} \rightarrow 2Fe^{2+}_{(aq)} + 4OH^-_{(aq)}$$

The standard emf for this process is 1.67 V in an acidic medium.

* Corresponding authors.
† Academia Sinica.
‡ Tamkang University.

The H^+ ions are supplied in part by the reaction of atmospheric carbon dioxide with water to form H_2CO_3. The Fe^{2+} ions formed at the anode are further oxidized by oxygen

$$4Fe^{2+}_{(aq)} + O_{2(g)} + (4+2x)H_2O_{(l)} \rightarrow$$
$$2Fe_2O_3 \cdot xH_2O_{(s)} + 8H^+_{(aq)}$$
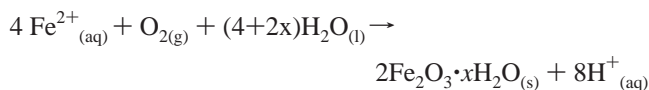
This hydrated form of iron (III) oxide is known as rust. The electric circuit is completed by the migration of the electrons and ions; this is the reason that rusting occurs so rapidly in salt water. In cold climates, salts (NaCl or $CaCl_2$) spread on roadways to melt ice and snow are a major cause of rust formation on automobiles.

All the above-mentioned processes take place in solution. An approach to understanding mechanisms of the reactions of Fe with H_2O and O_2 without and with the presence of protons can start from the study of these reactions in the gas phase. For such study, ab initio molecular orbital (MO) and density functional calculations of potential energy surfaces (PES) represent an invaluable tool. Once the gas-phase reaction mechanisms are understood by means of theoretical calculations and experimental measurements, a comparison can be made between the reactions in the gas phase and solution, and the

role of solvent and condensed phase effects can be better comprehended. The gas-phase studies provide first steps toward a more detailed understanding of the role of electronic structure in the more complex systems involved in solution chemistry.

Meanwhile, the gas phase reactions of iron atoms with water and oxygen are interesting by themselves. For instance, as was recently found by Kellogg and Itikura,[2] the Fe−O−H$_2$ PES is important for understanding the flame inhibition that occurs when iron compounds are added to a flame. Alternatively, the FeO radicals play a central role in controlling the layer of atomic Fe in the Earth's atmosphere.[3] Among others, FeO may undergo a reaction with molecular hydrogen, which is the reverse of Fe + H$_2$O. This reaction was recently studied experimentally[4] and was found to be very slow at 320 K. While the simple and fundamental reaction Fe + O$_2$ has been examined in argon matrices,[5−8] in the gas phase,[4,9−12] and by theoretical calculations,[8,11−15] the reactions in the Fe/H$_2$O/O$_2$ system are still far from being understood. Ground-state iron atoms are not reactive with O$_2$ in the gas phase near room temperature. Electronically excited iron atoms are expected to be more reactive; the reactions of laser-ablated Fe atoms and O$_2$ molecules in argon condensing on a 10 K surface were shown to produce FeOO and OFeO.[16] Annealing to 30 and 50 K gives cyclic FeO$_2$. The gas-phase reaction of Fe atoms with water at room temperature was studied by Mitchell and Hackett,[10] who found that the corresponding rate constant is low. However, little information is available about the mechanism of this fundamental reaction.

The present ab initio MO and DFT study is concentrated on the reaction pathways of iron atoms with H$_2$O as well as H$_2$S to elucidate the gas-phase reaction mechanisms. To analyze the role of acidic environment in the iron oxidation, we also consider the reaction mechanism in the presence of protons. To understand how the oxidation of Fe to Fe^{2+} can occur in the gas-phase, we compare thermochemistry and mechanisms of possible reactions involving iron atoms, water, H$^+$, and molecular oxygen.

2. Computational Details

We investigate the lowest quintet and triplet electronic state potential energy surfaces (PESs) for the Fe + H$_2$O → FeO + H$_2$ reaction. As will be shown below, the quintet state remains the ground electronic state along the reaction course. Therefore, we study only the quintet reaction pathway for the Fe + H$_2$S → FeS + H$_2$ reaction. On these surfaces, full geometry optimizations were run to locate all the stationary points at the unrestricted B3LYP/6-31G** level.[17,18] Harmonic vibrational frequencies were obtained at the same level in order to characterize the stationary points as minima or first-order saddle points, to obtain zero-point vibrational energy corrections (ZPE), and to generate force-constant data needed in the intrinsic reaction coordinate (IRC) calculation. The IRC method[19] was used to track minimum energy paths from transition structures to the corresponding minimum. A step size of 0.1 amu$^{1/2}$ bohr or larger was used in the IRC procedures. For comparison, geometries of some structures were also optimized at the unrestricted coupled cluster CCD/6-31G** level.[20]

The relative energies of various species were then refined using three levels of theory, B3LYP with the larger 6-311G** and 6-311+G(3df,2p) basis sets and the unrestricted coupled cluster CCSD(T)/6-311G**[20] at the B3LYP/6-31G** optimized geometries. The 6-311G* basis set for Fe available in the GAUSSIAN 98 program[21] includes valence triple-ζ s, p, and d basis function and a polarization f function. The Fe 6-311+G(3df)

basis set can be more correctly designated as 6-311+G(3fg) because it includes three polarization f functions and a g function in addition to the valence and diffuse s, p, and d basis functions. According to the literature,[22] the CCSD(T)/6-311G**//B3LYP/6-31G** level of theory can be considered as the most reliable in this study and superior with respect to B3LYP/6-311+G-(3df,2p)//B3LYP/6-31G**. However, in some cases, the B3LYP/6-311+G(3df,2p)//B3LYP/6-31G** method appeared to be superior as compared to CCSD(T)/6-311G**//B3LYP/6-31G**, which may be fortuitous or could be a result of CCSD(T) calculations performed on very contaminated UHF wave functions or due to the use of a moderate 6-311G** basis set. Meanwhile, in this study, the stability of UHF wave functions was checked for every structure, and only stable wave functions were used in UCCSD(T) calculations. In our discussion, we compare the performance of different methods.

Most of the ab initio calculations described here were carried out employing the Gaussian 98 program,[21] and for some of them, the MOLPRO 98 package[23] was used.

3. Results and Discussion

The ZPE corrected relative energies of various compounds in the Fe/H$_2$O/H$^+$ and Fe/O$_2$/H$^+$ system calculated at the B3LYP/6-31G**//B3LYP/6-31G**, B3LYP/6-311G**//B3LYP/6-31G**, B3LYP/6-311+G(3df,2p)//B3LYP/6-31G**, and CCSD(T)/6-311G**//B3LYP/6-31G** levels of theory are listed in Table 1. The energetics of various species in the Fe + H$_2$S → FeS + H$_2$ reaction is presented in Table 2. Table 3 shows vibrational frequencies calculated at the B3LYP/6-31G** level. The energy diagram, along the quintet and triplet reaction pathways of the Fe + H$_2$O → FeO + H$_2$, is shown in Figure 1. The energy diagrams for the Fe/H$_2$O/H$^+$ and [Fe/H$_2$O]$^{2+}$ systems are presented in Figure 2. The energy diagram for the Fe + H$_2$S → FeS + H$_2$ reaction in quintet electronic state is illustrated in Figure 3. The optimized geometries of various compounds are depicted in Figures 4−6. We use prefixes "q-" and "t-" to denote various species in the quintet and triplet electronic states, respectively.

Reaction Mechanism of Fe + H$_2$O. As seen in Figure 1, at the first stage of the reaction in quintet electronic state, the H$_2$O molecule attaches to the Fe atom (^{5}D, 3d^{6}4s^2) to form a q-Fe−OH$_2$ complex. The complex geometry is nonplanar and has C_s symmetry, with a long Fe−O bond of 2.175 Å (ca. with 1.604 and 1.746 Å in FeO and HFeOH, respectively). The structure of the H$_2$O fragment is nearly unchanged as compared to that of an isolated water molecule. The B3LYP/6-311+G(3df,2p) + ZPE(B3LYP/6-31G**) stabilization energy is 7.2 kcal/mol. However, at the CCSD(T)/6-311G**//B3LYP/6-31G** level, this complex does not exist and is 1.7 kcal/mol unstable with respect to the reactants. From the q-Fe−OH$_2$ complex (or directly from the reactants if the complex does not exist), the reaction proceeds by migration of one of the hydrogen atoms to form a planar nonlinear intermediate q-HFeOH via transition state q-TS1. From q-Fe−OH$_2$ to q-TS1, the H′OFe angle bends from 111.8° to 56.5°, and the hydrogen atom from the oxygen side of the molecule is shifted to a position above the Fe−O bond. The O−H′ distance increases to 1.435 Å, while a new Fe−H bond (1.624 Å) starts to form. The FeO bond (1.891 Å) also becomes stronger in the transition state. The barriers relative to q-Fe + H$_2$O calculated at the CCSD(T)/6-311G** and B3LYP/6-311+G(3df,2p) levels with ZPE are 32.7 and 14.8 kcal/mol, and the q-Fe + H$_2$O → q-HFeOH reaction is found to be exothermic by 26.2 and 34.2 kcal/mol, respectively. At different levels of theory (see Table 1), the barrier height varies

TABLE 1: ZPE Corrected Relative Energies (kcal/mol) Calculated at Different Levels of Theory for Various Compounds in the Fe/H$_2$O/H$^+$ and Fe/O$_2$/H$^+$ Systems

| species | ZPE[a] | B3LYP | | | CCSD(T) |
		6-31G**	6-311G**	6-311+G(3df,2p)	6-311G**
			Fe/H$_2$O		
q-Fe + H$_2$O	13.4	39.0	24.5	34.2	26.2
q-Fe−OH$_2$	14.4	31.2	22.3	27.0	27.9
q-TS1	10.3	49.3	51.7	49.0	58.9
q-HFeOH	10.7	0	0	0	0
q-TS2	9.0	61.1	66.2	58.1	75.5
q-FeO + H$_2$	7.8	48.3	53.9	46.3	62.4
t-Fe + H$_2$O	13.4	76.6	61.4	70.2	b
t-Fe−OH$_2$	14.4	60.8	48.1	42.6	39.9
t-TS1	10.9	70.5	63.1	60.4	75.9
t-HFeOH	11.1	27.9	28.5	30.7	22.1
t-TS2	9.3	78.5	89.7	80.4	92.7
t-OFe−H$_2$	9.3	62.0	88.5	77.4	89.4
t-FeO + H$_2$	7.1	70.2	70.6	74.2	81.6
			Fe/H$_2$O/H$^+$		
q-HFeOH + H$^+$	10.7	202.9	211.7	196.2	221.9
q-FeH$^+$ + H$_2$O	16.1	50.1	45.9	40.9	44.8
q-HFeOH$_2$$^+$	18.3	0	0	0	0
q-HFeOH$_2$ + TS	15.9	35.7	41.5	34.9	45.7
q-FeOH$^+$ + H$_2$	13.7	24.7	29.8	21.1	34.0
			Fe^{2+}/H$_2$O		
q-FeOH$^+$ + H$^+$	7.4	65.8	68.4	54.4	88.5
q-FeOH$^+$ + H$^+$ TS	7.9	100.3	103.7	102.0	136.4
q-FeOH$_2$$^{2+}$	15.3	0	0	0	0
q-Fe^{2+} + H$_2$O	13.4	49.5	39.3	34.4	55.0
q-FeO+2H$^+$	1.4	187.5	191.7	171.8	200.6
			Fe/O$_2$/H$^+$		
q-FeH$^+$ + O$_2$	5.1	49.4	35.8	41.2	14.9
q-HFeO$_2$$^+$	7.0	0	0	0	0
q-HFeO$_2$ + TS	5.8	18.5	18.3	14.4	17.0
q-FeOOH$^+$	10.5	−40.8	−44.1	−46.8	−52.9

^{a} Zero-point energies calculated at the B3LYP/6-31G** level. ^{b} Perturbative treatment of triple excitations in CCSD(T) fails to produce a reasonable result for triplet Fe atom. For instance, the correction for triple excitations is −0.03862 hartree for the triplet state, as compared to only −0.00181 hartree for the quintet. As a result, the CCSD/6-311G** calculated quintet-triplet energy gap of 23.8 kcal/mol reduces to 0.7 kcal/mol at the CCSD(T) level, inconsistent with the experimental quintet-triplet splitting of 34.2 kcal/mol (ref 24).
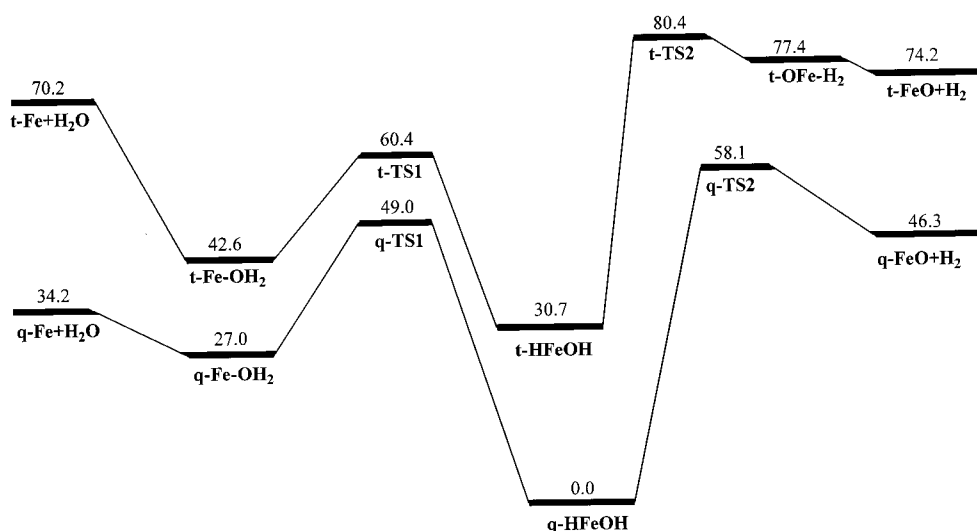

Figure 1. Potential energy diagram along the quintet and triplet reaction pathways of the Fe + H$_2$O → FeO + H$_2$ reaction calculated at the CCSD(T)/6-311G** and B3LYP/6-311+G(3df,2p) (in parentheses) levels of theory, including ZPE(B3LYP/6-31G**) at the B3LYP/6-31G** optimized geometries.

between 10.3 kcal/mol (B3LYP/6-31G**) and 32.7 kcal/mol (CCSD(T)/6-311G**). The IRC calculations at the B3LYP/6-31G** level of theory confirmed that q-TS1 connects the q-Fe−OH$_2$ complex and the planar nonlinear q-HFeOH molecule. It should be mentioned that Rollason and Plane[4] obtained a linear geometry of q-HFeOH at the B3LYP/6-311G level, which can be an artifact due to the absence of polarization functions in the basis set. The intermediate q-HFeOH can decompose directly

to q-FeO ($^5\Delta$) and H$_2$ via a planar transition state q-TS2. The Fe−O bond in q-TS2 (1.691 Å) becomes stronger, and the second hydrogen atom is shifted from the O-side of the molecule to a position above the Fe−O bond. A new H−H bond begins to form with the H−H distance of 0.922 Å. The transition state q-TS2 lies 75.5 (58.1) and 49.3 (23.9) kcal/mol higher in energy than q-HFeOH and the reactants, respectively, at the CCSD-(T)/6-311G** (B3LYP/6-311+G(3df,2p)) levels. The B3LYP/

TABLE 2: ZPE Corrected Relative Energies (kcal/mol) Calculated at Different Levels of Theory for Various Compounds in the Fe + H$_2$S → FeS + H$_2$ Reaction

species	ZPE[a]	B3LYP			CCSD(T)
		6-31G**	6-311G**	6-311+G(3df,2p)	6-311G**
q-Fe + H$_2$S	9.5	37.1	25.9	35.8	26.9
q-TS1(S)	8.1	43.5	40.7	37.8	51.5
q-HFeSH	8.3	0	0	0	0
q-TS2(S)	7.8	39.2	41.5	34.2	51.6
q-SFe−H$_2$	9.3	25.6	25.8	28.2	36.9
q-FeS + H$_2$	7.2	28.4	28.7	26.1	43.2

[a] Zero-point energies calculated at the B3LYP/6-31G** level.

TABLE 3: Vibrational Frequencies (cm^{-1}) of Various Quintet (q) and Triplet (t) Compounds in the Fe + H$_2$O and Fe + H$_2$S Reactions and in the Fe/H$_2$O/H$^+$ and Fe/O$_2$/H$^+$ Systems Calculated at the B3LYP/6-31G Level**

species	frequencies
q-Fe−OH$_2$	242, 343, 414, 1614, 3656, 3778
q-TS1	1154i, 473, 578, 831, 1560, 3756
q-HFeOH	210, 240, 406, 788, 1871, 3963
q-TS2	1241i, 645, 882, 1091, 1635, 2042
q-FeO	1008
t-Fe−OH$_2$	307, 360, 457, 1595, 3621, 3738
t-TS1	1147i, 552, 604, 1031, 1768, 3696
t-HFeOH	249, 369, 632, 781, 1863, 3894
t-TS2	895i, 704, 768, 928, 1770, 2331
t-OFe−H$_2$	160, 402, 646, 1107, 1864, 2344
t-FeO	493
q-FeH$^+$	1908
q-HFeOH$_2$$^+$	96, 129, 389, 409, 600, 1673, 1947,3743, 3824
q-HFeOH$_2$ + TS	1500i, 296, 631, 710, 995, 1191, 1741, 1804, 3787
q-FeOH$^+$	464, 836, 3845
q-FeOH$^+$ + H$^+$ TS	528i, 217, 277, 625, 744, 3662
q-Fe−OH$_2$$^{2+}$	546, 550, 733, 1668, 3558, 3615
q-HFeO$_2$$^+$	372, 380, 449, 605, 1197, 1889
q-HFeO$_2$ + TS	1240i, 415, 503, 687, 1068, 1363
q-FeOOH$^+$	280, 575, 681, 867, 1254, 3692
q-TS1(S)	358i, 382, 411, 872, 1358, 2662
q-HFeSH	170, 268, 385, 507, 1832, 2669
q-TS2(S)	1199i, 469, 739, 968, 1605, 1668
q-SFe−H$_2$	145, 211, 542, 564, 899, 4162
q-FeS	544

6-31G** IRC calculation confirmed the connections of the first-order saddle point q-TS2 with the q-HFeOH intermediate and the q-FeO + H$_2$ products. Overall, the Fe(^{5}D) + H$_2$O → FeO-($^5\Delta$) + H$_2$ reaction is calculated to be 12.1 kcal/mol endothermic at the B3LYP/6-311+G(3df,2p) level, which somewhat underestimates the experimental value of 18.5 kcal/mol.[24] On the other hand, CCSD(T)/6-311G** calculations give 36.2 kcal/mol for the reaction heat, twice higher than that in experiment. In summary, the reaction of the ground quintet electronic state iron atom with water should produce q-HFeOH, but the barrier is significant, and the reaction at room temperature should be slow. This conclusion agrees with the experimental finding by Mitchell and Hackett.[10] Further decomposition of q-HFeOH to FeO + H$_2$ is not likely to occur due to the high barrier at q-TS2. The reverse reaction, FeO + H$_2$, is found to have a barrier of 12−13 kcal/mol, which can explain the fact that no reaction was observed between FeO and molecular hydrogen at 320 K in the recent experimental study by Rollason and Plane.[4]

The Fe + H$_2$O → FeO + H$_2$ reaction in triplet electronic state has a mechanism similar to that of the quintet reaction. However, significant differences can be seen in the reaction energetics. Since the UHF wave function in the triplet state is subject to high-spin contamination, the UCCSD(T)/6-311G** results are expected to be less reliable, and we discuss below the B3LYP/6-311+G(3df,2p) energies. First, the Fe−OH$_2$ complex formation energy (27.6 kcal/mol for triplet) is significantly higher than that in the quintet state. The stability of t-Fe−
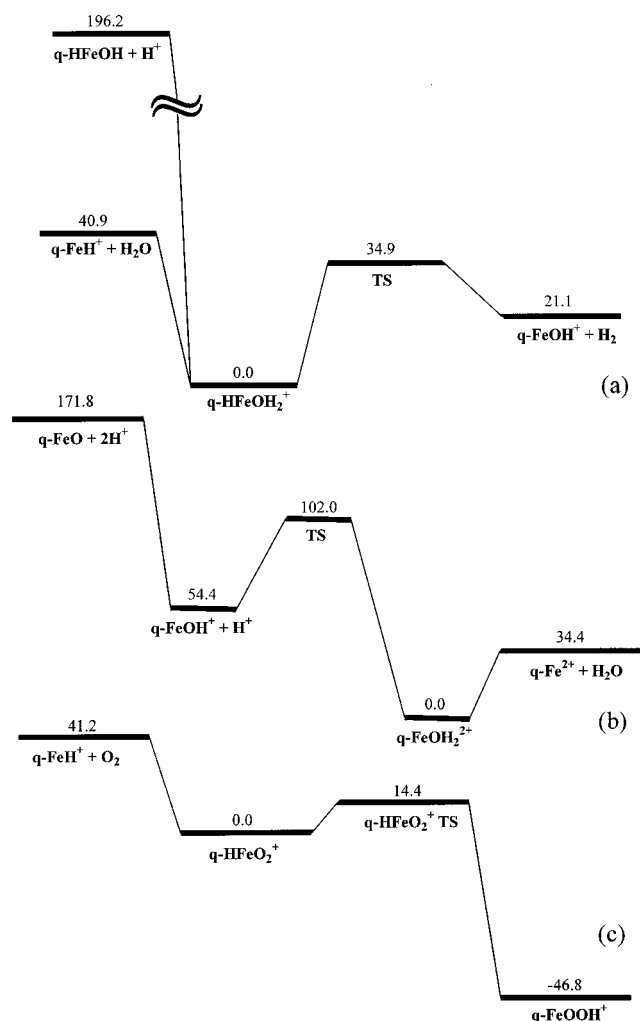

Figure 2. Potential energy diagrams for the Fe/H$_2$O/H$^+$ (a), [Fe/H$_2$O]$^{2+}$ (b), and Fe/O$_2$/H$^+$ (c) systems calculated at the CCSD(T)/6-311G** and B3LYP/6-311+G(3df,2p) (in parentheses) levels of theory, including ZPE(B3LYP/6-31G**) at the B3LYP/6-31G** optimized geometries.

OH$_2$ is also reflected in the much shorter Fe−O bond length (2.00 Å vs 2.18 Å in q-Fe−OH$_2$). The t-Fe−OH$_2$ complex lies 15.6 kcal/mol above the quintet complex. In isolated Fe atom, the lowest triplet state ^{3}F (3d^{7}4s^1) is 34.2 kcal/mol higher in energy than the ground ^{5}D state.[25] B3LYP/6-311+G(3df,2p) calculations reproduce the experimental quintet−triplet energy gap fairly well (36.0 kcal/mol). Lower-level B3LYP/6-31G** calculations indicate that in the triplet state, iron oxide can form a molecular complex with H$_2$ stabilized by 8.2 kcal/mol with regard to the separated products. However, this result is not reproduced at higher levels (see Table 1), and the t-OFe−H$_2$ complex is not expected to be stable. The transition state t-TS1 on the triplet PES lies lower in energy than the reactants, and the t-Fe + H$_2$O → t-HFeOH reaction is exothermic. This implies that the reaction of Fe atoms in excited triplet electronic state with water are expected to take place without activation and should be fast, much faster than the reaction of the ground-state iron atoms. One can also see from Figure 1 that the quintet and triplet potential energy surfaces in the Fe/H$_2$O system are not expected to cross. This is in contrast with the Ni + H$_2$O system, where the triplet and singlet surfaces do cross along the course of the reaction.[26,27] The existence of a low-lying excited singlet electronic state for the nickel atom and singlet−triplet intersystem crossings along the reaction pathways
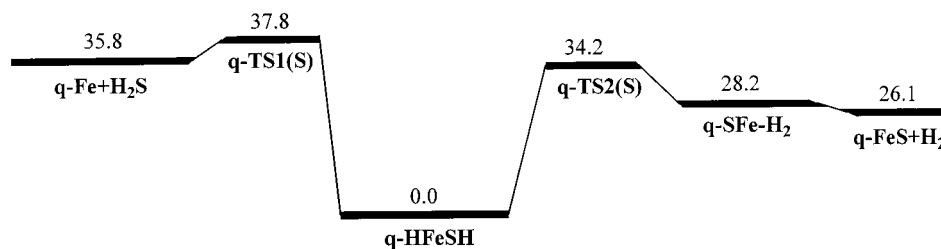
Figure 3. Potential energy diagram along the reaction pathways of the Fe + H_2S → FeS + H_2 reaction in quintet electronic state calculated at the CCSD(T)/6-311G** and B3LYP/6-311+G(3df,2p) (in parentheses) levels of theory, including ZPE(B3LYP/6-31G**) at the B3LYP/6-31G** optimized geometries.
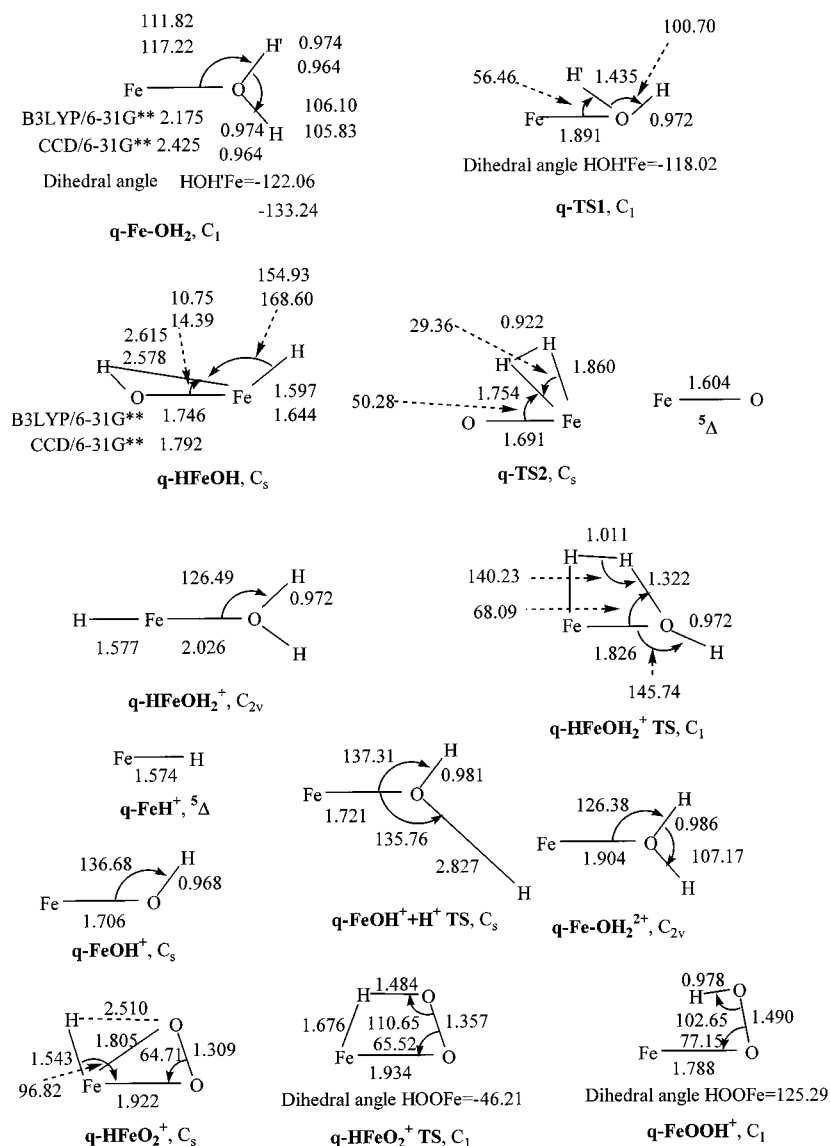

Figure 4. Optimized geometries (at the B3LYP/6-31G** level unless otherwise mentioned; bond lengths are in Å and bond angles are in deg) of various compounds in the Fe/H_2O/H^+ and Fe/O_2/H^+ systems in quintet electronic state.

significantly facilitates the Ni + H_2O reaction.[27] However, this is not the case for Fe + H_2O.

Fe + H_2O Reaction in Acidic Environment. While the initial steps of the Fe(^5D) + H_2O reaction leading to the formation of q-HFeOH can occur at elevated temperatures when the 15−33 kcal/mol barrier can be overcome, the formation of FeO is still unlikely. However, the reaction can go further in acidic environment, i.e., in the presence of protons. To illustrate this, we have studied the reaction mechanism of q-HFeOH with H^+. As seen in Figure 2, q-HFeOH can attach a proton, yielding

q-HFeOH$_2^+$ without activation barrier and with a large energy gain of 221.9 (196.2) kcal/mol at the CCSD(T)/6-311G** (B3LYP/6-311+G(3df,2p)) levels. The q-HFeOH$_2^+$ intermediate decomposes to release H_2 through an energy barrier of 45.7 (34.9) kcal/mol. Although in solution the energy of the q-HFeOH protonation is expected to be significantly smaller than 196−222 kcal/mol due to solvation of H^+ (the H_2O proton affinity is 165 kcal/mol[24]), the q-HFeOH + H^+ → q-HFeOH$_2^+$ → q-HFeOH$_2^+$ TS → q-FeOH$^+$ + H_2 is still expected to be feasible. The last reaction step is calculated to be 34.0 (21.1)
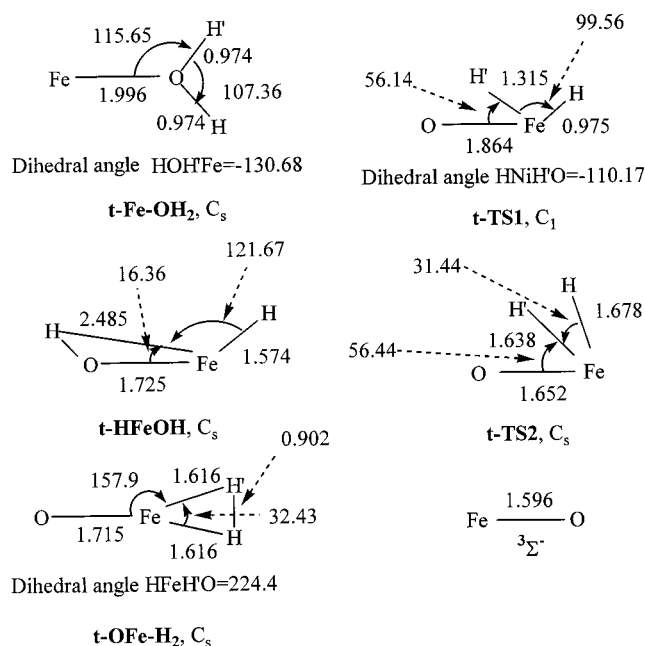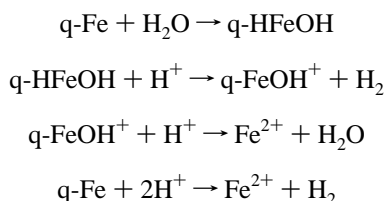
Figure 5. B3LYP/6-31G** optimized geometries (bond lengths are in Å and bond angles are in deg) of various species in the Fe + H$_2$O → FeO + H$_2$ reaction in triplet and singlet electronic states.

kcal/mol endothermic at CCSD(T)/6-311G** (B3LYP/6-311+G-(3df,2p)), but the overall reaction is highly exothermic and will apparently remain exothermic even in the presence of solvent. The B3LYP/6-31G** IRC calculation confirmed that the first-order saddle point q-HFeOH$_2$+ TS connects the q-HFeOH$_2$+ intermediate and the q-FeOH$^+$ + H$_2$ products.
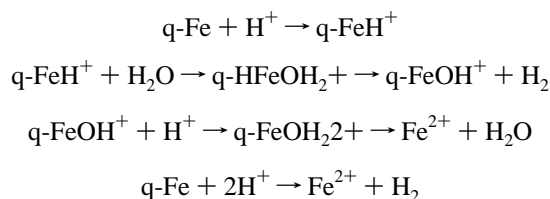
q-FeOH$^+$ is very unlikely to decompose to q-FeO + H$^+$ because this process requires 112−117 kcal/mol of energy. On the other hand, the q-FeOH$^+$ ion can add another proton to form q-FeOH$_2$$^{2+}$ with exothermicity of 88.5 and 54.4 kcal/mol at the CCSD(T)/6-311G** and B3LYP/6-311+G(3df,2p) levels, respectively. However, the second proton addition to FeOH$^+$ exhibits a high barrier of ~48 kcal/mol both at CCSD(T)/6-311G** and B3LYP/6-311+G(3df,2p) with ZPE, owing to the Coulombic repulsion. Therefore, this addition is not likely to occur in the gas phase at room temperature. In solution, protons and FeOH$^+$ can be solvated both in the reactants and transition state. This could result in shielding of the two positive charges and lead to a certain decrease of the barrier for their approach, since this barrier is mostly due to the Coulombic repulsion. On the next step, q-FeOH$_2$$^{2+}$ can dissociate to q-Fe^{2+} + H$_2$O without barrier and with endothermicity of 55.0 (34.4) kcal/mol at CCSD(T)/6-311G** (B3LYP/6-311+G(3df,2p)). The overall q-FeOH$^+$ + H$^+$ → q-FeOH$_2$2+ → q-Fe^{2+} + H$_2$O reaction is 33.5 (20.0) kcal/mol exothermic. The net reaction of iron atoms with water in acidic environment can be written as follows:

$$\text{q-Fe} + \text{H}_2\text{O} \rightarrow \text{q-HFeOH}$$

$$\text{q-HFeOH} + \text{H}^+ \rightarrow \text{q-FeOH}^+ + \text{H}_2$$

$$\text{q-FeOH}^+ + \text{H}^+ \rightarrow \text{Fe}^{2+} + \text{H}_2\text{O}$$

$$\text{q-Fe} + 2\text{H}^+ \rightarrow \text{Fe}^{2+} + \text{H}_2$$

In this reaction scheme, the critical barrier of 15−33 kcal/mol occurs at the q-Fe−OH$_2$ → q-TS1 → q-HFeOH reaction step, assuming that the proton addition to q-FeOH$^+$ is feasible in

solution. Under the conditions when this barrier can be overcome, the reaction can produce the Fe^{2+} ions.

Reaction of FeH$^+$ with Water. In acidic environment, neutral iron atoms can easily attach protons to form the FeH$^+$ molecule in quintet electronic state; the experimental proton affinity of Fe is as high as 180 kcal/mol[24] ca. with 185.5 kcal/mol obtained at the CCSD(T)/6-311+G(3df,2p) + ZPE(B3LYP/6-31G**) level. In turn, FeH$^+$ can readily react with water producing q-HFeOH$_2$$^+$ without any barrier. As seen in Table 1 and Figure 2, the exothermicity of the q-FeH$^+$ + H$_2$O → q-HFeOH$_2$$^+$ is 44.8 and 40.9 kcal/mol at the CCSD(T)/6-311G** and B3LYP/6-311+G(3df,2p) levels, respectively. In the previous section, we showed that the q-HFeOH$_2$$^+$ intermediate decomposes to q-FeOH$^+$ + H$_2$ with the barrier of 45.7 (34.9) kcal/mol. Therefore, the q-FeH$^+$ + H$_2$O → q-HFeOH$_2$+ → q-FeOH$^+$ + H$_2$ reaction is expected to take place with a very low barrier relative to that of the reactants or without activation and is expected to be fast. At the next step (which might be feasible only in solution), q-FeOH$^+$ would attach another proton and then dissociate to Fe^{2+} and water. The overall reaction mechanism in this case can be written as follows:

$$\text{q-Fe} + \text{H}^+ \rightarrow \text{q-FeH}^+$$

$$\text{q-FeH}^+ + \text{H}_2\text{O} \rightarrow \text{q-HFeOH}_2 + \rightarrow \text{q-FeOH}^+ + \text{H}_2$$

$$\text{q-FeOH}^+ + \text{H}^+ \rightarrow \text{q-FeOH}_2 2+ \rightarrow \text{Fe}^{2+} + \text{H}_2\text{O}$$

$$\text{q-Fe} + 2\text{H}^+ \rightarrow \text{Fe}^{2+} + \text{H}_2$$

Clearly, this reaction mechanism is preferable as compared to the mechanism which has the Fe + H$_2$O reaction as the first step.

Reaction of FeH$^+$ with Molecular Oxygen. The FeH$^+$ molecule can easily react not only with water but also with O$_2$. According to our calculations (see Figure 2c), FeH$^+$ and molecular oxygen combine together to produce a planar q-HFeO$_2$+ intermediate without barrier and with the energy gain of 14.9 (41.2) kcal/mol at CCSD(T)/6-311G** (B3LYP/6-311+G(3df,2p)). In q-HFeO$_2$+, the FeOO fragment represents a three-member ring, since the iron atom forms two bonds (1.922 and 1.805 Å) with oxygens. At the next reaction step, the hydrogen atom is shifted from Fe to the nearest oxygen to produce another q-FeOOH$^+$ intermediate. This step exhibits a barrier of 17.0 (14.4) kcal/mol. The corresponding transition state, q-HFeO$_2$+ TS, lies only 2.1 kcal/mol higher in energy than the reactants, q-FeH$^+$ + O$_2$, at the CCSD(T)/6-311G** level and 26.8 kcal/mol lower in energy than q-FeH$^+$ + O$_2$ at B3LYP/6-311+G(3df,2p). The q-HFeO$_2$+ → q-FeOOH$^+$ step is calculated to be 52.9 (46.8) kcal/mol exothermic, and the total exothermicity of the q-FeH$^+$ + O$_2$ → q-FeOOH$^+$ reaction is as high as 67.8 (88.0) kcal/mol. Thus, the reaction of FeH$^+$ with molecular oxygen is expected to take place with a low activation barrier or without barrier and to rapidly produce the q-FeOOH$^+$ ion. Once hydrated, this ion in the presence of protons can eventually dissociate to Fe^{2+} and hydrogen peroxide. The latter, in turn, can oxidize other iron atoms or undergo other chemical reactions in solution.

The FeH$^+$ + O$_2$ reaction is more facile than the reaction of FeH$^+$ with water due to higher overall exothermicity (67.8 kcal/mol vs 10.8 kcal/mol for FeH$^+$ + H$_2$O → FeOH$^+$ + H$_2$ as calculated at the CCSD(T)/6-311G** level) and a lower barrier for the intermediate reaction step (17.0 vs 45.7 kcal/mol). If the reactions take place in solution, the barrier heights for the individual steps can be rate-determining rather than the overall
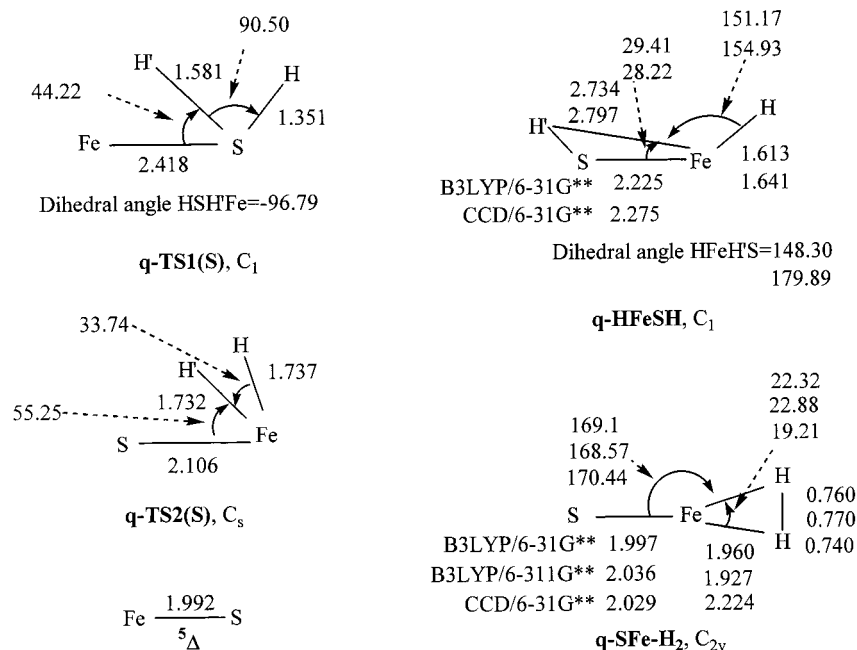
Figure 6. Optimized geometries (at the B3LYP/6-31G** level unless otherwise mentioned; bond lengths are in Å and bond angles are in deg) of various species in the Fe + H_2S → FeS + H_2 reaction in quintet electronic states.

reaction barrier, since intermediates can undergo a rapid collisional deactivation. In this view, the FeH^+ + O_2 → $FeOOH^+$ reaction is preferable not only with respect to FeH^+ + H_2O → $FeOH^+$ + H_2, but also Fe + H_2O → HFeOH, which has the highest reaction step barrier of 22.0−32.7 kcal/mol.

Reaction Mechanism of Fe + H_2S. In general, the mechanism of the Fe(^5D) + H_2S reaction is similar to that of Fe(^5D) + H_2O, but certain peculiarities exist. For instance, we could not locate a q-Fe−SH_2 complex; from the reactants, the reaction proceeds directly to the q-HFeSH intermediate via q-TS1(S). The barrier for the initial reaction step is only 2.0 kcal/mol at the B3LYP/6-311+G(3df,2p) level with ZPE, i.e., ~13 kcal/mol lower than that for the reaction with water calculated at the same level of theory. On the other hand, at CCSD(T)/6-311G**, the barrier is significant, 24.6 kcal/mol, but still ~8 kcal/mol lower than the CCSD(T)/6-311G** barrier for Fe + H_2O. The intermediate q-HFeSH has a nonplanar and nonlinear geometry and can dissociate to q-FeS + H_2 in two steps. First, a molecular q-SFe−H_2 complex is formed via q-TS2(S). This transition state is 3.6 kcal/mol lower energy than q-TS1(S) at B3LYP/6-311+G(3df,2p) but slightly, 0.1 kcal/mol, higher at CCSD(T)/6-311G**. The CCSD(T)/6-311G** (B3LYP/6-311+G(3df,2p)) calculated barrier is 51.6 (34.2) and 24.7 (8.1) kcal/mol relative to q-HFeSH and q-FeS + H_2, respectively. The q-HFeSH → q-SFe−H_2 reaction step is found to be endothermic by 36.9 and 28.2 kcal/mol at the CCSD(T)/6-311G** and B3LYP/6-311+G(3df,2p) levels, respectively. The q-SFe−H_2 complex is stable with respect to q-FeS and H_2 by 2−6 kcal/mol at B3LYP/6-31G**, B3LYP/6-311G**, and CCSD(T)/6-31G** levels but becomes unstable by 2.1 kcal/mol at B3LYP/6-311+G(3df,2p). The overall heat of the Fe-(^5D) + H_2S → FeS($^5Δ$) + H_2 reaction calculated at B3LYP/6-311+G(3df,2p) + ZPE is −9.7 kcal/mol (exothermic), while in experiment this reaction is 5.8 kcal/mol endothermic.[24] Noteworthy that only the CCSD(T)/6-311G** approximation gives a positive value for the reaction heat, 16.3 kcal/mol, though significantly overestimating the experimental reaction endothermicity. In experiment, free Fe atoms were found to be unreactive toward H_2S.[5] This indicates that the CCSD(T)/6-311G** barrier of ~25 kcal/mol is more reliable than the

B3LYP/6-311+G(3df,2p) value of 2.0 kcal/mol. At other levels of our calculations, the barrier height varies between 6.4 kcal/mol (B3LYP/6-31G**) and 14.8 kcal/mol (B3LYP/6-311G**). Upon the conditions when the barrier at q-TS1(S) can be overcome, the energized q-HFeSH complex can dissociate to q-FeS + H_2, since the energies of transition states q-TS2(S) and q-TS1(S) are similar. Thus, the Fe + H_2S reaction is more likely to produce FeS and molecular hydrogen than Fe + H_2O to yield FeO + H_2.

4. Conclusions

The reaction of free iron atoms with water in the ground quintet electronic state is shown to proceed by a possible formation of an Fe−OH_2 molecular complex stabilized by 7.2 kcal/mol with respect to the reactants at the B3LYP/6-311+G-(3df,2p)//B3LYP/6-31G** level but 1.7 kcal/mol unstable at CCSD(T)/6-311G**//B3LYP/6-31G**. The complex can isomerize to the HFeOH molecule overcoming the barrier of 22−32 kcal/mol (15−33 kcal/mol with respect to the reactants). Further decomposition of HFeOH to FeO and molecular hydrogen is hindered by a high barrier and is not likely to occur even at elevated temperatures.

In acidic environment, the HFeOH can sequentially react with two protons eventually producing Fe^{2+} + H_2O. On the other hand, in the presence of protons, iron atoms can easily attach H^+ with formation of the quintet FeH^+ molecules. The reaction of these molecules with water, q-FeH^+ + H_2O → q-$HFeOH_2^+$ → q-$FeOH^+$ + H_2, is exothermic and occurs without activation barrier. q-$FeOH^+$ may attach another proton in solution (only if positive charges of the two ions are shielded due to solvation to decrease a Coulomb repulsion barrier for their approach to each other) and dissociate to q-Fe^{2+} and H_2O. Thus, water molecules can assist oxidation of neutral iron atoms to Fe^{2+}. In this reaction scheme, two protons are converted into molecular hydrogen transferring their charge to Fe with the aid of H_2O. The FeH^+ can also readily react with molecular oxygen, yielding $HFeO_2^+$, which rearranges to the $FeOOH^+$ by the hydrogen shift with a barrier of ~14−17 kcal/mol. In solution, $FeOOH^+$ can eventually dissociate to Fe^{2+} and hydrogen peroxide. The FeH^+

$+ O_2 \rightarrow FeOOH^+$ reaction is predicted to be more facile than $FeH^+ + H_2O \rightarrow FeOH^+ + H_2$ because of much higher exothermicity and lower barrier for the intermediate reaction step.

The calculated barrier for the Fe + H₂O reaction is high enough to prevent the reaction at the room temperature, and the ground state Fe atoms react very slowly with H₂O in experiment.[10] Iron atoms are also unreactive toward molecular oxygen. The experimental endothermicity of the Fe + O₂ → FeO + O reaction is 20.3 kcal/mol,[24] slightly higher than that for Fe + H₂O → FeO + H₂. The presence of protons may assist the oxidation of iron atoms. The reaction mechanism involving sequential Fe (⁵D) + H⁺ → q-FeH⁺, q-FeH⁺ + H₂O → q-HFeOH₂+ → q-FeOH⁺ + H₂, q-FeOH⁺ + H⁺ → q-FeOH₂2+ → Fe²⁺ + H₂O reactions can oxidize Fe to Fe²⁺. However, this mechanism exhibits significant barriers for intermediate reaction steps, up to ~48 kcal/mol. Another possibility is the reaction of FeH⁺ with O₂, FeH⁺ + O₂ → HFeO₂+ → FeOOH⁺, followed by dissociation of the latter in solution. Of all reaction mechanisms considered in this study, we believe that the FeH⁺ + O₂ reaction may be most relevant to the first step of rusting, and the initial protonation of free iron atoms is crucial. It should be mentioned that Fe clusters were found experimentally to be much more reactive toward small molecules than the free atoms,[9,10] so the reactions of the clusters with water and oxygen can also contribute to the rusting process. Also, in nature, rusting is slow and usually occurs on the inhomogeneous sites. To form free iron atoms or clusters, the lattice energy has to be overcome, which may not be easy even in the presence of protons. Furthermore, rusting may occur by different mechanisms at gas−solid and liquid−solid (aqueous) interfaces.

The calculations showed that electronically excited triplet iron atoms are more reactive with H₂O than the ground-state iron atom. The reaction proceeds by the following mechanism: Fe + H₂O → Fe−OH₂ → HFeOH → OFe−H₂ → FeO + H₂. The pathway leading to triplet HFeOH is exothermic, with the transition state lying lower in energy than the reactants. No triplet-quintet intersystem crossing was found along the reaction pathway.

The reaction mechanism for Fe + H₂S in ground quintet electronic state is quite similar to that for the reaction with water. However, the critical barrier for the formation of the HFeSH intermediate is notably lower than the corresponding barrier for the H₂O reaction. The barrier for the second reaction step is comparable with the barrier for the initial step, so HFeSH is likely to decompose to FeS and molecular hydrogen. Fe and H₂S do not form a molecular complex. Overall, the Fe + H₂S → FeS + H₂ reaction is much less endothermic than Fe + H₂O → FeO + H₂. Because of the reduced endothermicity and lower reaction barriers, the reaction of iron atoms with H₂S is more likely to yield iron sulfide and molecular hydrogen, than the reaction with water to produce FeO + H₂.

References and Notes

(1) Zumdahl, S. S. *Chemical Principles*, 3rd ed.; Houghton Mifflin: Boston, 1998.

(2) Kellogg, C. B.; Itikura, K. K. *J. Phys. Chem. A* **1999**, *103*, 1150.

(3) (a) Kane, T. J.; Gardner, C. S. *J. Geophys. Res.* **1993**, *98*, 16875. (b) Alpers, M.; Höffner, J.; von Zahn, U. *J. Geophys. Res.* **1994**, *99*, 13971. (c) Helmer, M.; Plane, J. M. C.; Qian, J.; Gardner, C. S. *J. Geophys. Res.* **1993**, *98*, 10913. (d) Plane, J. M. C.; Cox, R. M.; Rollason, R. J. *Adv. Space Res.* **1999**, *24*, 1559.

(4) Rollason, R. J.; Plane, J. M. C. *Phys. Chem. Chem. Phys.* **2000**, *2*, 2335.

(5) Abramowitz, S.; Acquista, N.; Levin, I. W. *Chem. Phys. Lett.* **1977**, *50*, 423.

(6) Chang, S.; Blyholder, G.; Fernandez, J. *Inorg. Chem.* **1981**, *20*, 2813.

(7) Serebrennikov, L. V. *Vestn. Mosk. Univers. Ser. 2, Khim.* **1988**, *29*, 451.

(8) Chertihin, G. V.; Saffel, W.; Yustein, J. T.; Andrews, L.; Neurock, M.; Ricca, A.; Bauschlicher, Jr., C. W. *J. Phys. Chem.* **1996**, *100*, 5261.

(9) Whetten, R. L.; Cox, D. M.; Trevor, D. J.; Kaldor, A. *J. Phys. Chem.* **1985**, *89*, 566.

(10) Mitchell, S. A.; Hackett, P. A. *J. Chem. Phys.* **1990**, *93*, 7822.

(11) Helmer, M.; Plane, J. M. C. *J. Chem. Soc., Faraday Trans.* **1994**, *90*, 395.

(12) Schröder, D.; Fiedler, A.; Schwarz, J.; Schwarz, H. *Inorg. Chem.* **1994**, *33*, 5094.

(13) Blyholder, G.; Head, J.; Ruette, F. *Inorg. Chem.* **1982**, *21*, 1539.

(14) Lyne, P. D.; Mingos, D. M. P.; Ziegler, T.; Downs, A. J. *Inorg. Chem.* **1993**, *32*, 4785.

(15) Cao, Z.; Duran, M.; Solà, M. *Chem. Phys. Lett.* **1997**, *274*, 411.

(16) Andrews, L.; Chertihin, G. V.; Ricca, A.; Bauschlicher, Jr., C. W. *J. Am. Chem. Soc.* **1996**, *118*, 467.

(17) Becke, A. D. *J. Chem. Phys.* **1993**, *98*, 5648.

(18) Lee, C.; Yang, W.; Parr, R. G. *Phys. Rev.* **1988**, *B 37*, 785.

(19) Gonzales, C.; Schlegel, H. B. *J. Chem. Phys.* **1989**, *90*, 2154.

(20) (a) Purvis, G. D.; Bartlett, R. J. *J. Chem. Phys.* **1982**, *76*, 1910. (b) Hampel, C.; Peterson, K. A.; Werner, H.-J. *Chem. Phys. Lett.* **1992**, *190*, 1. (c) Knowles, P. J.; Hampel, C.; Werner, H.-J. *J. Chem. Phys.* **1994**, *99*, 5219. (d) Deegan, M. J. O.; Knowles, P. J. *Chem. Phys. Lett.* **1994**, *227*, 321.

(21) Frisch, M. J.; Trucks, G. W.; Schlegel, H. B.; Scuseria, G. E.; Robb, M. A.; Cheeseman, J. R.; Zakrzewski, V. G.; Montgomery, J. A., Jr.; Stratmann, R. E.; Burant, J. C.; Dapprich, S.; Millam, J. M.; Daniels, A. D.; Kudin, K. N.; Strain, M. C.; Farkas, O.; Tomasi, J.; Barone, V.; Cossi, M.; Cammi, R.; Mennucci, B.; Pomelli, C.; Adamo, C.; Clifford, S.; Ochterski, J.; Petersson, G. A.; Ayala, P. Y.; Cui, Q.; Morokuma, K.; Malick, D. K.; Rabuck, A. D.; Raghavachari, K.; Foresman, J. B.; Cioslowski, J.; Ortiz, J. V.; Baboul, A. G.; Stefanov, B. B.; Liu, G.; Liashenko, A.; Piskorz, P.; Komaromi, I.; Gomperts, R.; Martin, R. L.; Fox, D. J.; Keith, T.; Al-Laham, M. A.; Peng, C. Y.; Nanayakkara, A.; Gonzalez, C.; Challacombe, M.; Gill, P. M. W.; Johnson, B.; Chen, W.; Wong, M. W.; Andres, J. L.; Head-Gordon, M.; Replogle, E. S.; Pople, J. A. *Gaussian 98*, Revision A.7; Gaussian, Inc.: Pittsburgh, PA, 1998.

(22) Torrent, M.; Solà, M.; Frenking, G. *Chem. Rev.* **2000**, *100*, 439.

(23) MOLPRO is a package of ab initio programs written by H.-J. Werner and P. J. Knowles, with contributions from J. Almlöf, R. D. Amos, M. J. O. Deegan, S. T. Elbert, C. Hampel, W. Meyer, K. Peterson, R. Pitzer, A. J. Stone, P. R. Taylor, and R. Lindh.

(24) *NIST Chemistry Webbook*, NIST Standard Reference Data Base Number 69, February 2000 Release (http://webbook.nist.gov/chemistry/).

(25) Moore, C. *Atomic Energy Levels as Derived from the Analyses of Optical Spectra*; NIST: Washington, 1971.

(26) Hwang, D.-Y.; Mebel, A. M. *J. Phys. Chem.*, submitted for publication.

(27) Mitchell, S. A.; Blitz, A.; Siegbahn, P. E. M.; Svensson, M. *J. Chem. Phys.* **1994**, *100*, 423.